

# Tomographic Image Reconstruction in Noisy and Limited Data Settings.

Syed Tabish Abbas

International Institute of Information Technology, Hyderabad

*syed.abbas@research.iiit.ac.in*

July 1, 2016

# Problem Statement and Contributions

- We investigate the tomographic reconstruction under 2 scenarios
  - Noisy Data case.
  - Limited Data case.and consider the following questions.
- In linear Radon transform, does reconstruction lattice play a role in quality of reconstructed image?
- How to reconstruct an image under limited view circular Radon Transform: the Circular arc Radon transform?
- How to remove the artifacts which arise in the Circular arc Radon transform due to the limited view?

# Problem Statement and Contributions

- We investigate the tomographic reconstruction under 2 scenarios
  - Noisy Data case.
  - Limited Data case.

and consider the following questions.

- In linear Radon transform, does reconstruction lattice play a role in quality of reconstructed image?
- How to reconstruct an image under limited view circular Radon Transform: the Circular arc Radon transform?
- How to remove the artifacts which arise in the Circular arc Radon transform due to the limited view?

# Problem Statement and Contributions

- We investigate the tomographic reconstruction under 2 scenarios
  - Noisy Data case.
  - Limited Data case.

and consider the following questions.

- In linear Radon transform, does reconstruction lattice play a role in quality of reconstructed image?
- How to reconstruct an image under limited view circular Radon Transform: the Circular arc Radon transform?
- How to remove the artifacts which arise in the Circular arc Radon transform due to the limited view?

# Problem Statement and Contributions

- We investigate the tomographic reconstruction under 2 scenarios
    - Noisy Data case.
    - Limited Data case.
- and consider the following questions.
- In linear Radon transform, does reconstruction lattice play a role in quality of reconstructed image?
  - How to reconstruct an image under limited view circular Radon Transform: the Circular arc Radon transform?
  - How to remove the artifacts which arise in the Circular arc Radon transform due to the limited view?

# Problem Statement and Contributions

- We investigate the tomographic reconstruction under 2 scenarios
  - Noisy Data case.
  - Limited Data case.and consider the following questions.
- In linear Radon transform, does reconstruction lattice play a role in quality of reconstructed image?
- How to reconstruct an image under limited view circular Radon Transform: the Circular arc Radon transform?
- How to remove the artifacts which arise in the Circular arc Radon transform due to the limited view?

# Problem Statement and Contributions

- We investigate the tomographic reconstruction under 2 scenarios
  - Noisy Data case.
  - Limited Data case.and consider the following questions.
- In linear Radon transform, does reconstruction lattice play a role in quality of reconstructed image?
- How to reconstruct an image under limited view circular Radon Transform: the Circular arc Radon transform?
- How to remove the artifacts which arise in the Circular arc Radon transform due to the limited view?

# Problem Statement and Contributions

- We investigate the tomographic reconstruction under 2 scenarios
  - Noisy Data case.
  - Limited Data case.and consider the following questions.
- In linear Radon transform, does reconstruction lattice play a role in quality of reconstructed image?
- How to reconstruct an image under limited view circular Radon Transform: the Circular arc Radon transform?
- How to remove the artifacts which arise in the Circular arc Radon transform due to the limited view?

# Reconstruction onto Hexagonal Lattices.

In linear Radon transform, does reconstruction lattice play a role in quality of reconstructed image?

# Positron Emission Tomography(PET)

- Positron Emission Tomography(PET) is an invasive, nuclear imaging technique involves injecting the patient with a radioactive material(*tracer*)

# Positron Emission Tomography(PET)

- Positron Emission Tomography(PET) is an invasive, nuclear imaging technique involves injecting the patient with a radioactive material(*tracer*)
- PET imaging allows collecting metabolic information about different tissues.

# Positron Emission Tomography(PET)

- Positron Emission Tomography(PET) is an invasive, nuclear imaging technique involves injecting the patient with a radioactive material(*tracer*)
- PET imaging allows collecting metabolic information about different tissues.
- Due to physics of imaging process, PET scans are very noisy.

# Positron Emission Tomography(PET)

- Positron Emission Tomography(PET) is an invasive, nuclear imaging technique involves injecting the patient with a radioactive material(*tracer*)
- PET imaging allows collecting metabolic information about different tissues.
- Due to physics of imaging process, PET scans are very noisy.

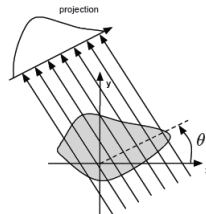


Figure: Forward Projection.

# PET Image Reconstruction

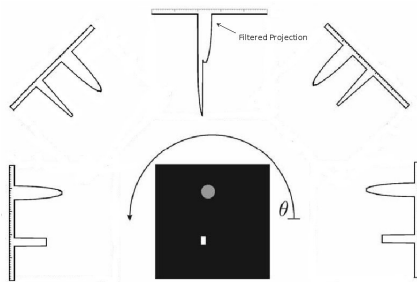
- PET Images are *reconstructed* from noisy sinogram data by essentially inverting the forward emission process.

# PET Image Reconstruction

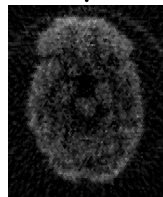
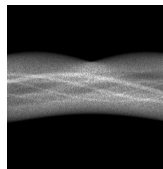
- PET Images are *reconstructed* from noisy sinogram data by essentially inverting the forward emission process.
- An approximate inversion is achieved by *high pass filtered back projection*.

# PET Image Reconstruction

- PET Images are *reconstructed* from noisy sinogram data by essentially inverting the forward emission process.
- An approximate inversion is achieved by *high pass filtered back projection*.



# Handling Noisy Data



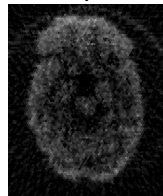
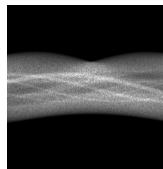
Reconstructed  
Image

1

<sup>1</sup>Herman, '80, <sup>2</sup>Fessler, '00 <sup>3</sup> Valiollahzadeh, '13

# Handling Noisy Data

- More sophisticated methods, like algebraic inversion<sup>1</sup>, Statistical inversion<sup>2</sup>, etc. have also been proposed



Reconstructed  
Image

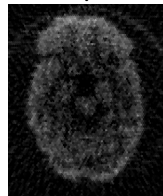
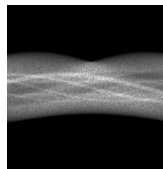
1

---

<sup>1</sup>Herman, '80, <sup>2</sup>Fessler, '00 <sup>3</sup> Valiollahzadeh, '13

# Handling Noisy Data

- More sophisticated methods, like algebraic inversion<sup>1</sup>, Statistical inversion<sup>2</sup>, etc. have also been proposed
- Other methods, follow a two step process of reconstruction followed by denoising<sup>3</sup>.



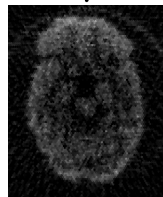
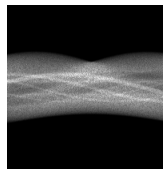
Reconstructed  
Image

1

<sup>1</sup>Herman, '80, <sup>2</sup>Fessler, '00 <sup>3</sup> Valiollahzadeh, '13

# Handling Noisy Data

- More sophisticated methods, like algebraic inversion<sup>1</sup>, Statistical inversion<sup>2</sup>, etc. have also been proposed
- Other methods, follow a two step process of reconstruction followed by denoising<sup>3</sup>.
- *Reconstruction onto a different lattice has received very little attention.*



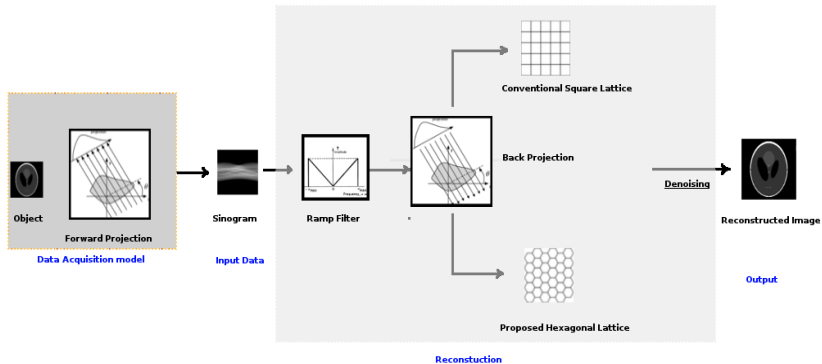
Reconstructed  
Image

1

<sup>1</sup>Herman, '80, <sup>2</sup>Fessler, '00 <sup>3</sup> Valiollahzadeh, '13

# Our Pipeline

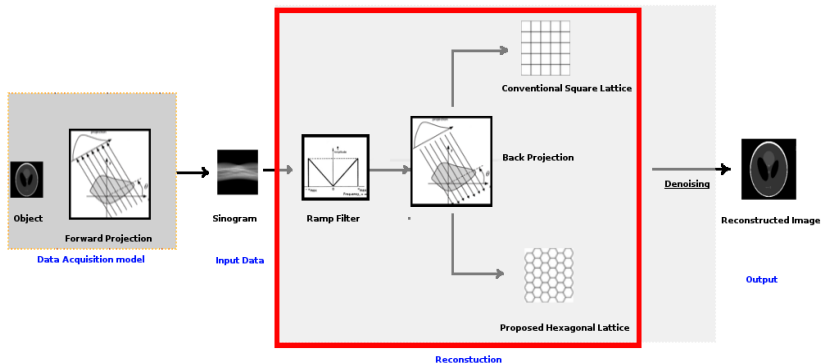
We propose a 2 step reconstruction process onto Hexagonal lattice:



# Our Pipeline

We propose a 2 step reconstruction process onto Hexagonal lattice:

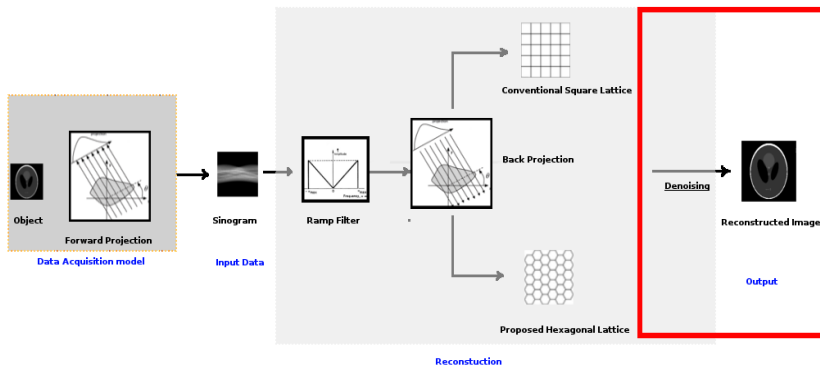
→ *Step 1: Noisy Reconstruction using Filtered Back Projection.*



# Our Pipeline

We propose a 2 step reconstruction process onto Hexagonal lattice:

- *Step 1: Noisy Reconstruction using Filtered Back Projection.*
- *Step 2: Denoising using a sparse dictionary learned for the noisy image.*



# Tiling of Euclidean Plane

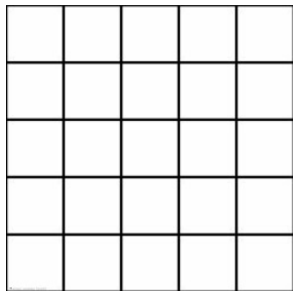


Figure: Square Tiling of Euclidean Plane

# Tiling of Euclidean Plane

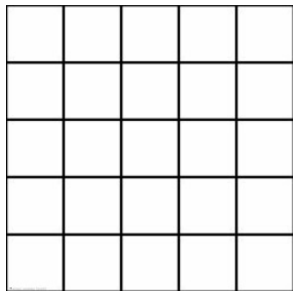


Figure: Square Tiling of Euclidean Plane

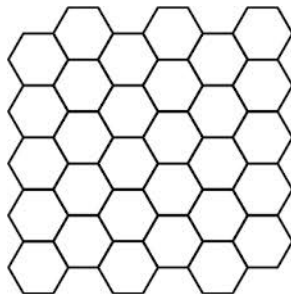


Figure: Hexagonal Tiling of Euclidean Plane

# Tiling of Euclidean Plane

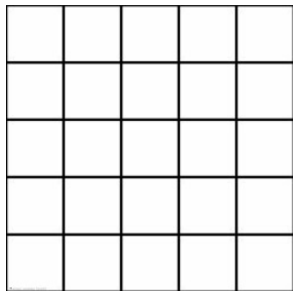


Figure: Square Tiling of Euclidean Plane

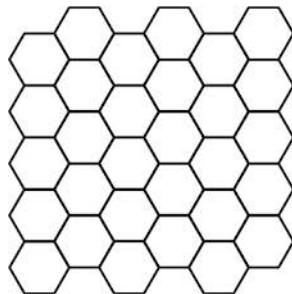


Figure: Hexagonal Tiling of Euclidean Plane

- ✓ *Packing density.*
- ✓ *Larger, symmetric neighbourhood*

# Tiling of Euclidean Plane

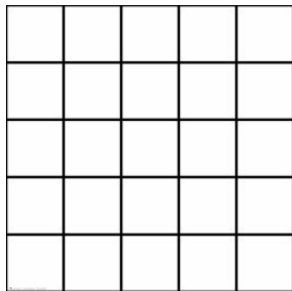


Figure: Square Tiling of Euclidean Plane

- ✓ *Packing density.*
- ✓ *Larger, symmetric neighbourhood*

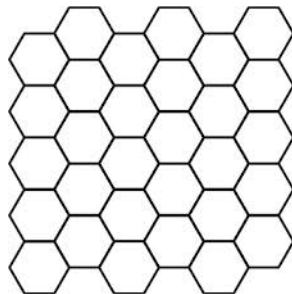
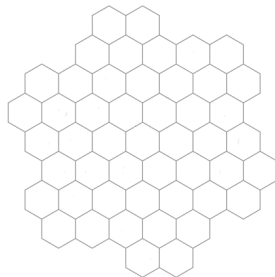


Figure: Hexagonal Tiling of Euclidean Plane

- ✗ Irrational Coordinates

# Addressing Hexagonal Lattices



2

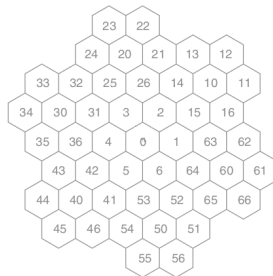
**Figure:** Addressing Hexagonal Lattice

---

<sup>2</sup>L Middleton and J Sivaswamy, 2006.

# Addressing Hexagonal Lattices

→ Use base 7 indices



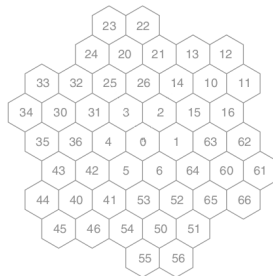
2

Figure: Addressing Hexagonal Lattice

<sup>2</sup>L Middleton and J Sivaswamy, 2006.

# Addressing Hexagonal Lattices

- Use base 7 indices
- Start numbering from center and move out spirally.



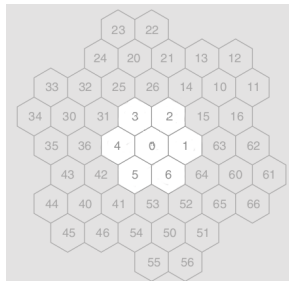
2

Figure: Addressing Hexagonal Lattice

<sup>2</sup>L Middleton and J Sivaswamy, 2006.

# Addressing Hexagonal Lattices

- Use base 7 indices
- Start numbering from center and move out spirally.



2

Figure: Addressing Hexagonal Lattice

<sup>2</sup>L Middleton and J Sivaswamy, 2006.

# Hexagonal Patch and vectorization

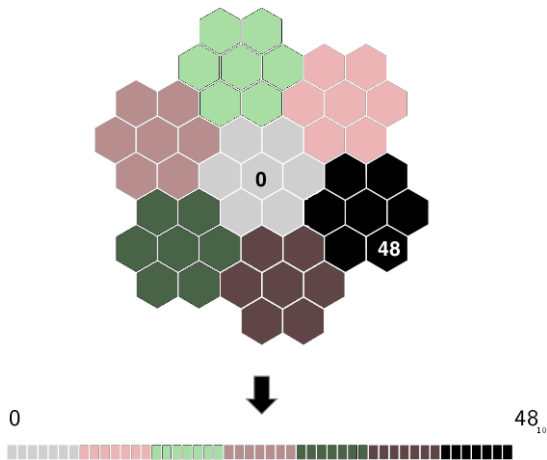


Figure: Hexagonal Patch of order 2

# Hexagonal Patch and vectorization

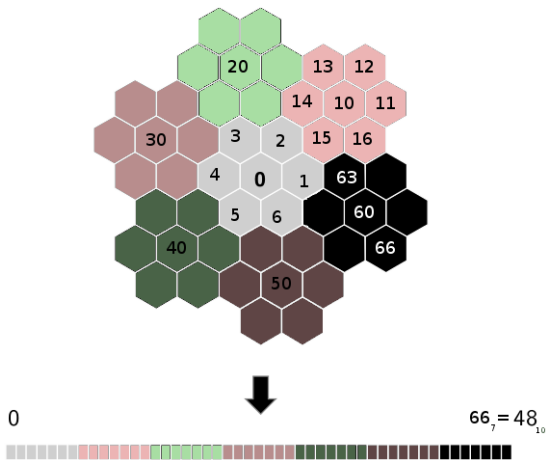
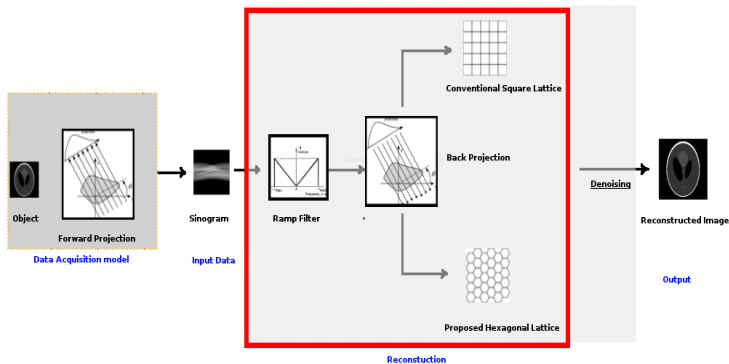


Figure: Hexagonal Patch of order 2

# Our Pipeline

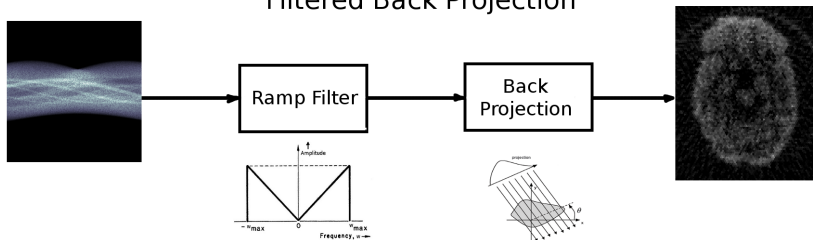
We propose a 2 step reconstruction process onto Hexagonal lattice:

- *Step 1: Noisy Reconstruction using Filtered Back Projection.*
- *Step 2: Denoising using a sparse dictionary learned for the noisy image.*

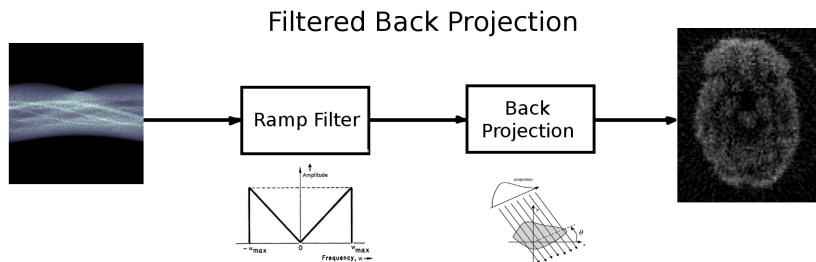


# Filtered Back-Projection (FBP)

## Filtered Back Projection

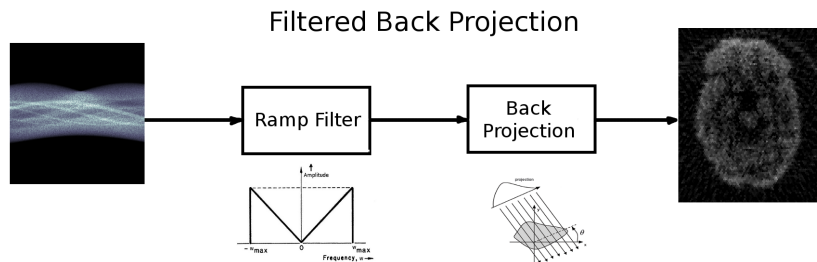


# Filtered Back-Projection (FBP)



X Image reconstruction (especially in nuclear modalities) is very noisy.

# Filtered Back-Projection (FBP)



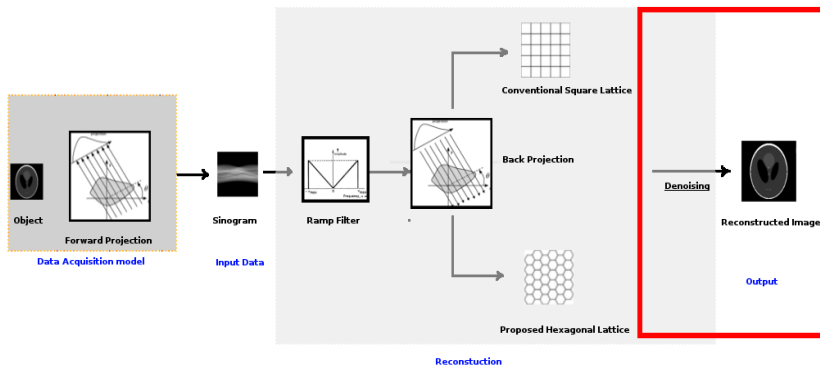
- ✗ Image reconstruction (especially in nuclear modalities) is very noisy.
- ✓ Back-projection (and also other reconstruction methods) allows a choice of reconstruction lattice.

# Our Pipeline

We propose a 2 step reconstruction process onto Hexagonal lattice:

✓ *Step 1: Noisy Reconstruction using Filtered Back Projection.*

→ *Step 2: Denoising using a sparse dictionary learned for the noisy image.*



# Dictionary based denoising

- Learn a dictionary of patches of size 49 (a level 2 patch).

3

---

<sup>3</sup>M Elad and M Aharon, 2006

# Dictionary based denoising

- Learn a dictionary of patches of size 49 (a level 2 patch).
- Use the learned dictionary for Denoising.

- Learn a dictionary of patches of size 49 (a level 2 patch).
- Use the learned dictionary for Denoising.
- Dictionary is learned by solving the following optimization problem.

$$\min_{D \in \mathcal{C}, \alpha \in \mathcal{R}^{k \times n}} \frac{1}{2} \| \mathbf{X} - \mathbf{D}\alpha \|_F^2 + \lambda \| \alpha \|_{1,1}$$

$$\mathcal{C} = \{ \mathbf{D} \in \mathcal{R}^{m \times k} \text{ s.t. } \forall j = 1, \dots, k, \| d_j^T \|_2 \leq 1 \}$$

3

# Dictionary based denoising

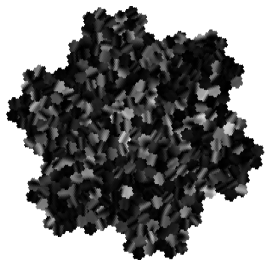


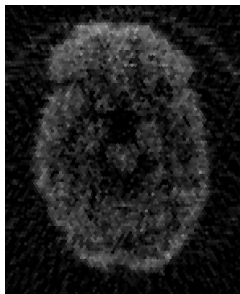
Figure: Sample Dictionary atoms

- Learn a dictionary of patches of size 49 (a level 2 patch).
- Use the learned dictionary for Denoising.
- Dictionary is learned by solving the following optimization problem.

$$\min_{D \in \mathcal{C}, \alpha \in \mathcal{R}^{k \times n}} \frac{1}{2} \| \mathbf{X} - \mathbf{D}\alpha \|_F^2 + \lambda \| \alpha \|_{1,1}$$

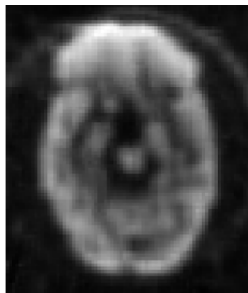
$$\mathcal{C} = \{ \mathbf{D} \in \mathcal{R}^{m \times k} \text{ s.t. } \forall j = 1, \dots, k, \| d_j^T \|_2 \leq 1 \}$$

3

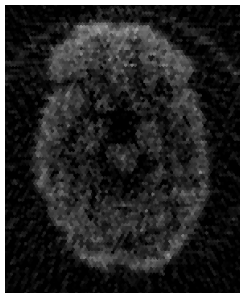


Noisy Image

# Qualitative Results

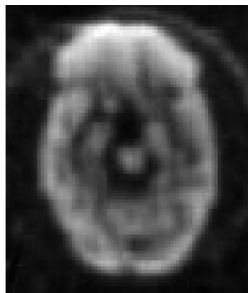


Square lattice

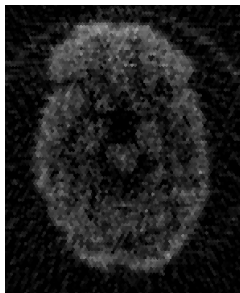


Noisy Image

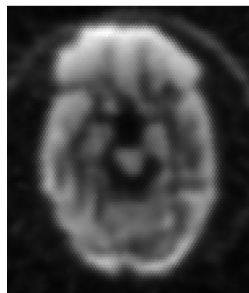
# Qualitative Results



Square lattice

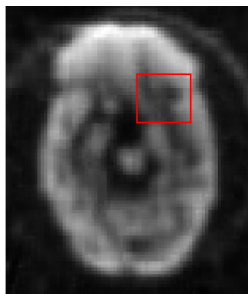


Noisy Image

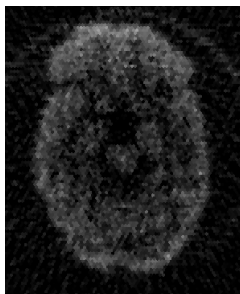


Hexagonal lattice

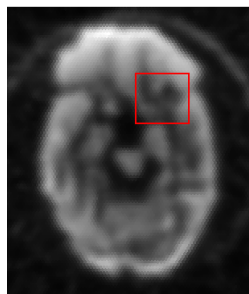
# Qualitative Results



Square lattice



Noisy Image

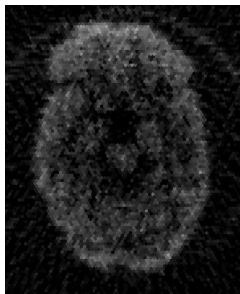


Hexagonal lattice

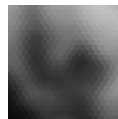
# Qualitative Results



Square lattice

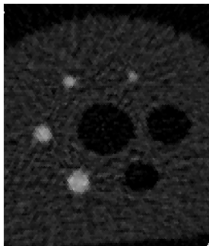


Noisy Image



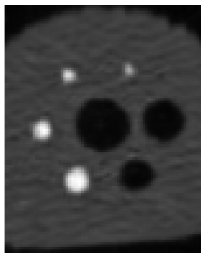
Hexagonal lattice

# Qualitative Results

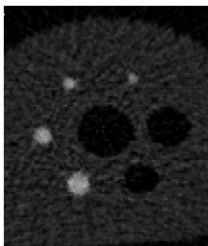


Noisy Image

# Qualitative Results

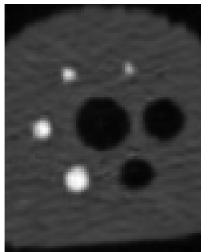


Square lattice

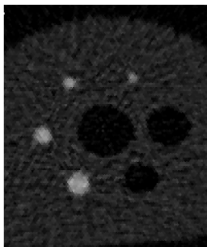


Noisy Image

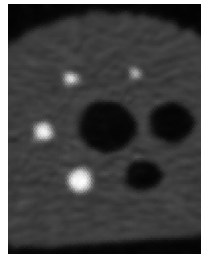
# Qualitative Results



Square lattice

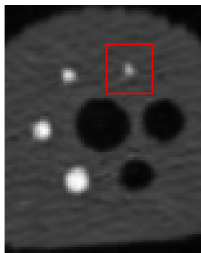


Noisy Image

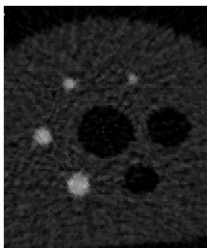


Hexagonal lattice

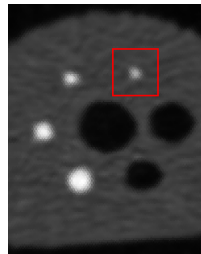
# Qualitative Results



Square lattice



Noisy Image

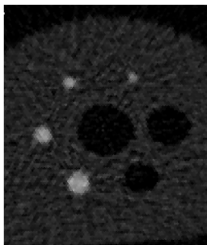


Hexagonal lattice

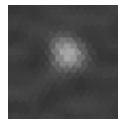
# Qualitative Results



Square lattice



Noisy Image



Hexagonal lattice

# Quantitative Results

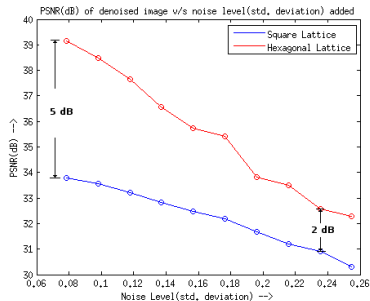


Figure: PSNR Comparison

# Quantitative Results

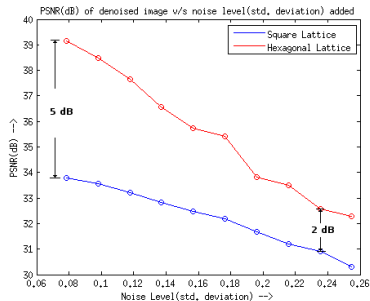


Figure: PSNR Comparison

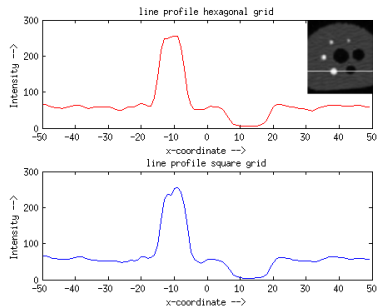


Figure: Line Profile

# Summary & Future Work

- ✓ We Proposed that the change of lattice can improve the reconstruction quality of PET images.
- ✓ The change in lattice improves both the quality and fidelity of the final denoised image.
- ✓ Include the noise model in the denoising step.
- ✓ Provide an analytical explanation for the improvement in reconstruction.

# Summary & Future Work

- ✓ We Proposed that the change of lattice can improve the reconstruction quality of PET images.
- ✓ The change in lattice improves both the quality and fidelity of the final denoised image.
- ✓ Include the noise model in the denoising step.
- ✓ Provide an analytical explanation for the improvement in reconstruction.

# Summary & Future Work

- ✓ We Proposed that the change of lattice can improve the reconstruction quality of PET images.
- ✓ The change in lattice improves both the quality and fidelity of the final denoised image.
- ✓ **Include the noise model in the denoising step.**
- ✓ Provide an analytical explanation for the improvement in reconstruction.

# Summary & Future Work

- ✓ We Proposed that the change of lattice can improve the reconstruction quality of PET images.
- ✓ The change in lattice improves both the quality and fidelity of the final denoised image.
- ✓ Include the noise model in the denoising step.
- ✓ Provide an analytical explanation for the improvement in reconstruction.

# Reconstruction In Limited View Scenario

How to reconstruct an image under limited view circular Radon Transform: the Circular arc Radon transform?

# Imaging setup

- **Type:** Photoacoustic type sensors where source of excitement is EM waves and measurement is acoustic waves.

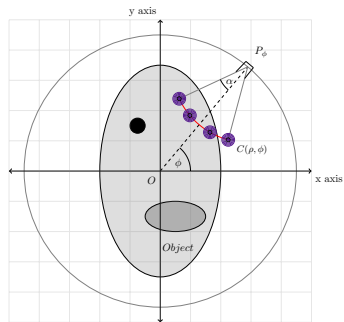


Figure: Measurement Setup.

# Imaging setup

- **Type:** Photoacoustic type sensors where source of excitement is EM waves and measurement is acoustic waves.
- **Geometry:** The sensors are assumed to be along a circle at points  $P_\phi$ .

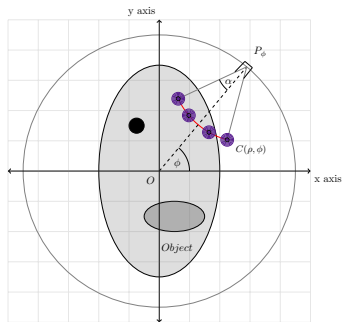


Figure: Measurement Setup.

# Imaging setup

- **Type:** Photoacoustic type sensors where source of excitement is EM waves and measurement is acoustic waves.
- **Geometry:** The sensors are assumed to be along a circle at points  $P_\phi$ .
- **Sensor Structure:** Each sensor is assumed to have a *limited conical view* equal to  $\alpha$

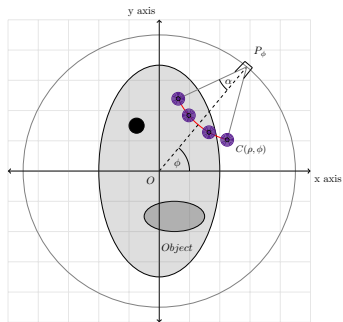


Figure: Measurement Setup.

# Imaging setup

- **Type:** Photoacoustic type sensors where source of excitement is EM waves and measurement is acoustic waves.
- **Geometry:** The sensors are assumed to be along a circle at points  $P_\phi$ .
- **Sensor Structure:** Each sensor is assumed to have a *limited conical view* equal to  $\alpha$

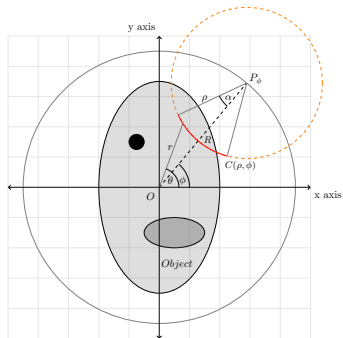


Figure: Measurement Setup.

# Mathematical Model

We define Circular arc Radon(CAR) Transform  $g^\alpha$  of a function  $f$  as follows

$$g^\alpha(\rho, \phi) = \int_{A_\alpha(\rho, \phi)} f(r, \theta) ds \quad (1)$$

where  $\alpha$  is the view angle and  $s$  is the arc length measure.

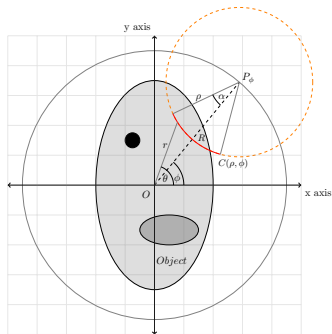


Figure: Measurement Setup.

# Mathematical Model

We define Circular arc Radon(CAR) Transform  $g^\alpha$  of a function  $f$  as follows

$$g^\alpha(\rho, \phi) = \int_{A_\alpha(\rho, \phi)}^{\text{Object}} f(r, \theta) ds \quad (1)$$

where  $\alpha$  is the view angle and  $s$  is the arc length measure.

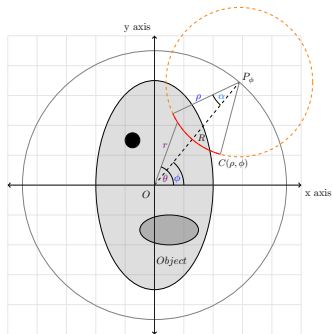


Figure: Measurement Setup.



# Mathematical Model

We define Circular arc Radon(CAR) Transform  $g^\alpha$  of a function  $f$  as follows

$$\underbrace{g^\alpha(\rho, \phi)}_{\text{Measured Data}} = \int_{A_\alpha(\rho, \phi)}^{\text{Object}} f(r, \theta) ds \quad (1)$$

where  $\alpha$  is the view angle and  $s$  is the arc length measure.

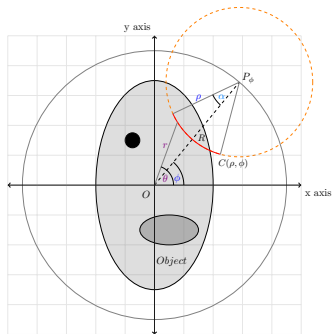


Figure: Measurement Setup.

# CAR Transform: Back projection based inversion

An approximate inversion of the transform may be done using an algorithm based on Backprojection, such that

# CAR Transform: Back projection based inversion

An approximate inversion of the transform may be done using an algorithm based on Backprojection, such that

$$f(x, y) = \int_0^{2\pi} g(\rho, \sqrt{(x - \cos \phi)^2 + (y - \sin \phi)^2}) d\phi$$

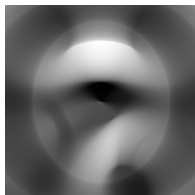
# CAR Transform: Back projection based inversion

An approximate inversion of the transform may be done using an algorithm based on Backprojection, such that

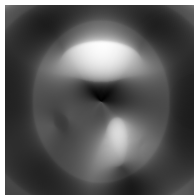
$$f(x, y) = \int_0^{2\pi} g(\rho, \sqrt{(x - \cos \phi)^2 + (y - \sin \phi)^2}) d\phi$$



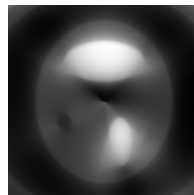
(a) Original  
Phantom



(b)  $\alpha = 5$



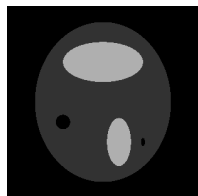
(c)  $\alpha = 17$



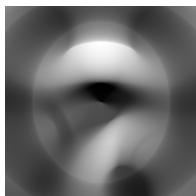
(d)  $\alpha = 21$

Examples of image reconstructions using a naïve Backprojection Algorithm

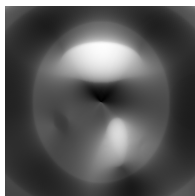
# CAR Transform: Back projection based inversion



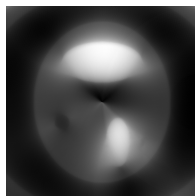
(a) Original  
Phantom



(b)  $\alpha = 5$



(c)  $\alpha = 17$

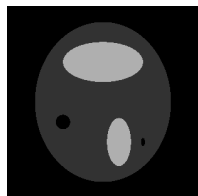


(d)  $\alpha = 21$

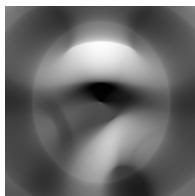
Examples of image reconstructions using a naïve Backprojection Algorithm

- The BP based algorithm is an approximate inversion and leads to lot of artifacts as well as blurring.

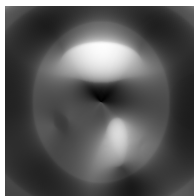
# CAR Transform: Back projection based inversion



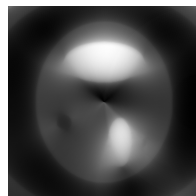
(a) Original Phantom



(b)  $\alpha = 5$



(c)  $\alpha = 17$

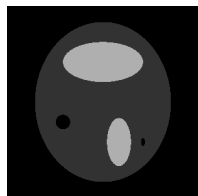


(d)  $\alpha = 21$

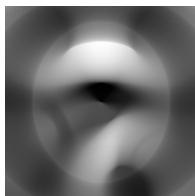
Examples of image reconstructions using a naïve Backprojection Algorithm

- The BP based algorithm is an approximate inversion and leads to lot of artifacts as well as blurring.
- Due the form of transform, it is non-trivial to derive the exact form of the filter.

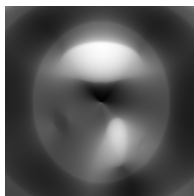
# CAR Transform: Back projection based inversion



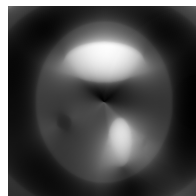
(a) Original  
Phantom



(b)  $\alpha = 5$



(c)  $\alpha = 17$



(d)  $\alpha = 21$

Examples of image reconstructions using a naïve Backprojection Algorithm

- The BP based algorithm is an approximate inversion and leads to lot of artifacts as well as blurring.
- Due the form of transform, it is non-trivial to derive the exact form of the filter.
- To improve the quality of reconstruction, we adopt a **Fourier series** based solution.

# CAR Transform: Fourier Series based analysis

$$g^\alpha(\rho, \phi) = \int_{A_\alpha(\rho, \phi)} f(r, \theta) ds$$

Since both  $f$ ,  $g$  are  $2\pi$  periodic in angular variable, we may expand them into their Fourier series such that,

# CAR Transform: Fourier Series based analysis

$$g^\alpha(\rho, \phi) = \int_{A_\alpha(\rho, \phi)} f(r, \theta) ds$$

Since both  $f$ ,  $g$  are  $2\pi$  periodic in angular variable, we may expand them into their Fourier series such that, then,

$$\sum_{n=-\infty}^{\infty} g_n^\alpha(\rho) e^{in\phi} = \sum_{n=-\infty}^{\infty} \int_{A_\alpha(\rho, \phi)} f_n(r) e^{in\theta} d\theta.$$

# CAR Transform: Fourier Series based analysis

On Simplifying and equating the Fourier coefficients, the equation reduces to

$$g_n^\alpha(\rho) = \int_{R - \sqrt{R^2 + \rho^2 - 2\rho R \cos \alpha}}^{\rho} \frac{K_n(\rho, u)}{\sqrt{\rho - u}} F_n(u) du$$

where

$$F_n(u) = f_n(R - u)$$

and

$$K_n(\rho, u) = \frac{2\rho(R - u) T_n \left[ \frac{(R - u)^2 + R^2 - \rho^2}{2R(R - u)} \right]}{\sqrt{(u + \rho)(2R + \rho - u)(2R - \rho - u)}}. \quad (2)$$

where,  $T_n(x) = \cos(n \cos^{-1}(x))$

# CAR Transform: Fourier Series based analysis

On Simplifying and equating the Fourier coefficients, the equation reduces to

$$g_n^\alpha(\rho) = \int_{R - \sqrt{R^2 + \rho^2 - 2\rho R \cos \alpha}}^{\rho} \frac{K_n(\rho, u)}{\sqrt{\rho - u}} F_n(u) du$$

where

$$F_n(u) = f_n(R - u)$$

and

$$K_n(\rho, u) = \frac{2\rho(R - u) T_n \left[ \frac{(R - u)^2 + R^2 - \rho^2}{2R(R - u)} \right]}{\sqrt{(u + \rho)(2R + \rho - u)(2R - \rho - u)}}. \quad (2)$$

where,  $T_n(x) = \cos(n \cos^{-1}(x))$

# CAR Transform: Fourier Series based analysis

On Simplifying and equating the Fourier coefficients, the equation reduces to

$$g_n^\alpha(\rho) = \int_{R - \sqrt{R^2 + \rho^2 - 2\rho R \cos \alpha}}^{\rho} \frac{K_n(\rho, u)}{\sqrt{\rho - u}} F_n(u) du$$

where

$$F_n(u) = f_n(R - u)$$

and

$$K_n(\rho, u) = \frac{2\rho(R - u) T_n \left[ \frac{(R - u)^2 + R^2 - \rho^2}{2R(R - u)} \right]}{\sqrt{(u + \rho)(2R + \rho - u)(2R - \rho - u)}}. \quad (2)$$

where,  $T_n(x) = \cos(n \cos^{-1}(x))$

# CAR Transform: Integral equation

$$g_n^\alpha(\rho) = \int_{R - \sqrt{R^2 + \rho^2 - 2\rho R \cos \alpha}}^{\rho} \frac{K_n(\rho, u)}{\sqrt{\rho - u}} F_n(u) du \quad (3)$$

- The equation is a non-standard Volterra integral equation of first kind with a weakly singular kernel.

# CAR Transform: Integral equation

$$g_n^\alpha(\rho) = \int_{R - \sqrt{R^2 + \rho^2 - 2\rho R \cos \alpha}}^{\rho} \overbrace{\frac{K_n(\rho, u)}{\sqrt{\rho - u}}}^{\text{Singular Kernel}} F_n(u) du \quad (3)$$

- The equation is a non-standard Volterra integral equation of first kind with a **weakly singular** kernel.

# CAR Transform: Integral equation

$$g_n^\alpha(\rho) = \int_{R-\sqrt{R^2+\rho^2-2\rho R \cos \alpha}}^{\rho} \overbrace{\frac{K_n(\rho, u)}{\sqrt{\rho-u}}}^{\text{Singular Kernel}} F_n(u) du \quad (3)$$

The diagram shows a box labeled "Functions" with two blue arrows. One arrow points to the upper limit of the integral,  $\rho$ , and the other points to the lower limit,  $R-\sqrt{R^2+\rho^2-2\rho R \cos \alpha}$ .

- The equation is a **non-standard** Volterra integral equation of first kind with a **weakly singular** kernel.

# CAR Transform: Integral equation

$$g_n^\alpha(\rho) = \int_{R-\sqrt{R^2+\rho^2-2\rho R \cos \alpha}}^{\rho} \overbrace{\frac{K_n(\rho, u)}{\sqrt{\rho-u}}}^{\text{Singular Kernel}} F_n(u) du \quad (3)$$

The diagram shows a box labeled "Functions" with two blue arrows pointing to the integrand and the upper limit of the integral in the equation above.

- The equation is a **non-standard** Volterra integral equation of first kind with a **weakly singular** kernel.
- ☹ The exact (closed form) solution of such an equation is not known.

# CAR Transform: Integral equation

$$g_n^\alpha(\rho) = \int_{R-\sqrt{R^2+\rho^2-2\rho R \cos \alpha}}^{\rho} \overbrace{\frac{K_n(\rho, u)}{\sqrt{\rho-u}}}^{\text{Singular Kernel}} F_n(u) du \quad (3)$$

The diagram shows a box labeled "Functions" with two blue arrows pointing to the integrand and the upper limit of the integral. The upper limit is labeled with a red  $\rho$ . The kernel is labeled "Singular Kernel" with a bracket above it.

- The equation is a **non-standard** Volterra integral equation of first kind with a **weakly singular** kernel.
- ☹ The exact (closed form) solution of such an equation is not known.
- ☺ A direct numerical solution of the equation does not require closed form solution.

# Discrete CAR Transform

$$g_n^\alpha(\rho) = \int_{R - \sqrt{R^2 + \rho^2 - 2\rho R \cos \alpha}}^{\rho} \frac{K_n(\rho, u)}{\sqrt{\rho - u}} F_n(u) du.$$

$$g_n^\alpha(\rho_k) = \sum_{q=1}^k \int_{\rho_{q-1}}^{\rho_q} \frac{F_n(u) K_n(\rho, u)}{\sqrt{\rho - u}} du.$$

# Discrete CAR Transform

$$g_n^\alpha(\rho_k) = \sum_{q=1}^k \int_{\rho_{q-1}}^{\rho_q} \frac{F_n(u) K_n(\rho, u)}{\sqrt{\rho - u}} du.$$

Approximating the integrand as a linear function over each interval  $[\rho_{q-1}, \rho_q]$ , and integrating we get

$$g_n(\rho_k) = \sqrt{h} \left\{ \sum_{q=1}^k b_{kq} K_n(\rho_k, \rho_q) F_n(\rho_q) \right\}$$

# Discrete CAR Transform

$$g_n^\alpha(\rho_k) = \sum_{q=1}^k \int_{\rho_{q-1}}^{\rho_q} \frac{F_n(u) K_n(\rho, u)}{\sqrt{\rho - u}} du.$$

Approximating the integrand as a linear function over each interval  $[\rho_{q-1}, \rho_q]$ , and integrating we get

$$g_n(\rho_k) = \sqrt{h} \left\{ \sum_{q=l}^k b_{kq} K_n(\rho_k, \rho_q) F_n(\rho_q) \right\}$$

where

$$b_{kq} = \begin{cases} \frac{4}{3} \left\{ (k-q+1)^{\frac{3}{2}} + \frac{4}{3}(k-q)^{\frac{3}{2}} + 2(k-q)^{\frac{1}{2}} \right\} & q = l \\ \frac{4}{3} \left( (k-q+1)^{\frac{3}{2}} - 2(k-q)^{\frac{3}{2}} + (k-q-1)^{\frac{3}{2}} \right) & q = l+1, \dots, k-1. \\ \frac{4}{3} & q = k. \end{cases}$$

and  $l = \max \left( 0, \left\lfloor R - \sqrt{R^2 + \rho_k^2 - 2\rho_k R \cos \alpha} \right\rfloor \right)$  where  $\lfloor x \rfloor$  is the greatest integer less than equal to  $x$ .

# Discrete CAR Transform

$$g_n(\rho_k) = \sqrt{h} \left\{ \sum_{q=1}^k b_{kq} K_n(\rho_k, \rho_q) F_n(\rho_q) \right\}$$

The previous equation can be written in the matrix form as

$$\mathbf{g}_n^\alpha = \mathbf{B}_n \mathbf{F}_n \quad (4)$$

# Discrete CAR Transform

$$g_n(\rho_k) = \sqrt{h} \left\{ \sum_{q=l}^k b_{kq} K_n(\rho_k, \rho_q) F_n(\rho_q) \right\}$$

The previous equation can be written in the matrix form as

$$\mathbf{g}_n^\alpha = B_n F_n \quad (4)$$

where

$$\mathbf{g}_n^\alpha = \begin{pmatrix} g_n^\alpha(\rho_0) \\ \vdots \\ g_n^\alpha(\rho_{M-1}) \end{pmatrix} \quad F_n = \begin{pmatrix} F_n(\rho_0) \\ \vdots \\ F_n(\rho_{M-1}) \end{pmatrix}.$$

# Discrete CAR Transform

$$g_n(\rho_k) = \sqrt{h} \left\{ \sum_{q=l}^k b_{kq} K_n(\rho_k, \rho_q) F_n(\rho_q) \right\}$$

The previous equation can be written in the matrix form as

$$\mathbf{g}_n^\alpha = B_n F_n \quad (4)$$

where

$$\mathbf{g}_n^\alpha = \begin{pmatrix} g_n^\alpha(\rho_0) \\ \vdots \\ g_n^\alpha(\rho_{M-1}) \end{pmatrix} \quad F_n = \begin{pmatrix} F_n(\rho_0) \\ \vdots \\ F_n(\rho_{M-1}) \end{pmatrix}.$$

- Matrix  $B_n$  **lower triangular** matrix which is a piecewise linear, discrete approximation of the integral in Equation (3).

# Discrete CAR Transform

The previous equation can be written in the matrix form as

$$\mathbf{g}_n^\alpha = B_n F_n \quad (4)$$

where

$$\mathbf{g}_n^\alpha = \begin{pmatrix} g_n^\alpha(\rho_0) \\ \vdots \\ g_n^\alpha(\rho_{M-1}) \end{pmatrix} \quad F_n = \begin{pmatrix} F_n(\rho_0) \\ \vdots \\ F_n(\rho_{M-1}) \end{pmatrix}.$$

- Matrix  $B_n$  **lower triangular** matrix which is a piecewise linear, discrete approximation of the integral in Equation (3).
- Diagonal entries of  $B_n$ ,  $b_{ii} = \frac{4}{3}\sqrt{h} \neq 0$ , hence the matrix is **invertible**.

# Numerical inversion of CAR Transform.

$$g_n^\alpha = B_n F_n$$

- ☺ Matrix  $B_n$  **lower triangular** matrix which is a piecewise linear, discrete approximation of the integral in Equation (3).
- ☺ Diagonal entries of  $B_n$ ,  $b_{ii} = \frac{4}{3}\sqrt{h} \neq 0$ , hence the matrix is **invertible**.
- ☹ The matrix is  $B_n$  has a **high condition number** ( $\mathcal{O}(10^{15})$ ), hence direct inversion is unstable.

# Numerical inversion of CAR Transform.

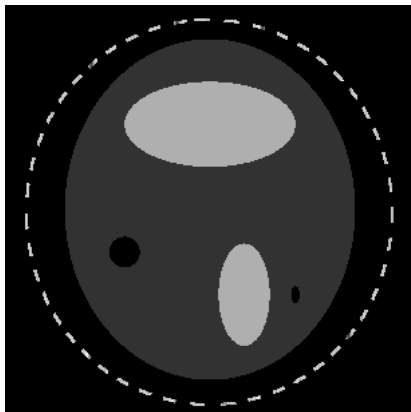
$$g_n^\alpha = B_n F_n$$

- ☺ Matrix  $B_n$  **lower triangular** matrix which is a piecewise linear, discrete approximation of the integral in Equation (3).
- ☺ Diagonal entries of  $B_n$ ,  $b_{ii} = \frac{4}{3}\sqrt{h} \neq 0$ , hence the matrix is **invertible**.
- ☹ The matrix is  $B_n$  has a **high condition number** ( $\mathcal{O}(10^{15})$ ), hence direct inversion is unstable.

We use a Truncated SVD based  $r$ -rank inverse ( $r < M$ ) such that,

$$F_n \approx B_{n,r}^{-1} g_n^\alpha$$

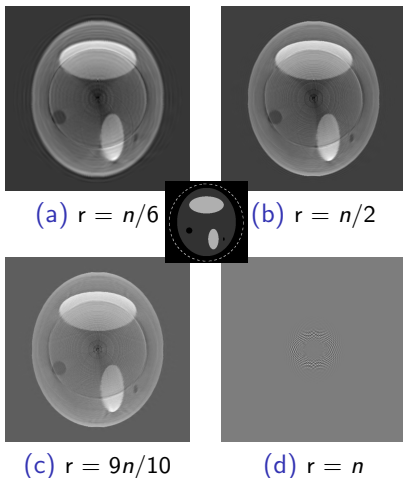
# Experiments and Results: Effect of Rank



original phantom ( $f$ ) used in experiments.

# Experiments and Results: Effect of Rank

- Full rank inversion is expected to be unstable.

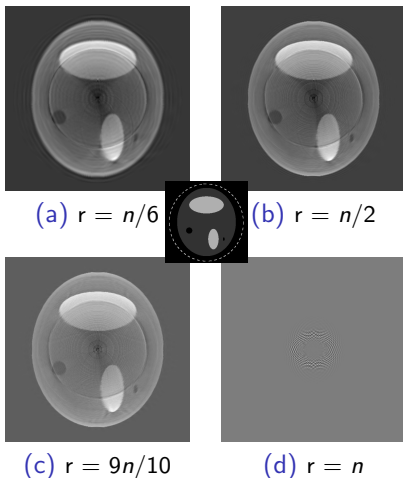


Effect of rank  $r$  of matrix  $B_{n,r}$  on the reconstruction

quality.  $n = 300$

# Experiments and Results: Effect of Rank

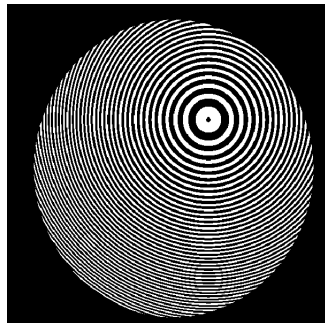
- Full rank inversion is expected to be unstable.
- If the rank  $r$  is set to be too low reconstructed image is expected to have ringing artifacts.



Effect of rank  $r$  of matrix  $B_{n,r}$  on the reconstruction

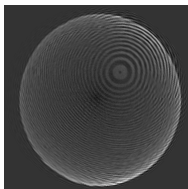
quality.  $n = 300$

# Experiments and Results: Choosing Rank

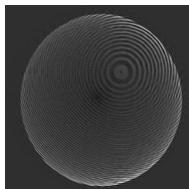


original phantom ( $f$ ) used in experiments.

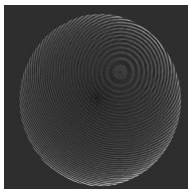
# Experiments and Results: Choosing Rank



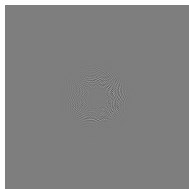
(a)  $r = n/3$



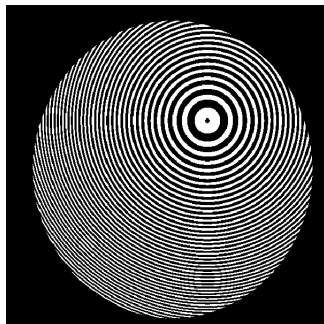
(b)  $r = n/2$



(c)  $r = 9n/10$



(d)  $r = n$

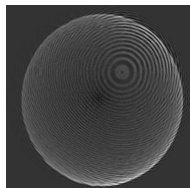


original phantom ( $f$ ) used in experiments.

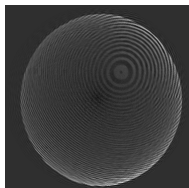
Effect of rank  $r$  of matrix  $B_{n,r}$  on the reconstruction

quality.  $n = 300$

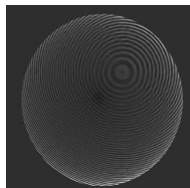
# Experiments and Results: Choosing Rank



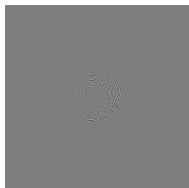
(a)  $r = n/3$



(b)  $r = n/2$



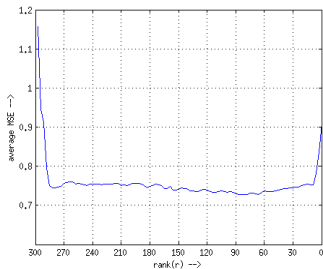
(c)  $r = 9n/10$



(d)  $r = n$

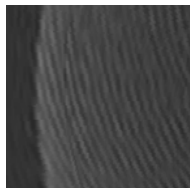
Effect of rank  $r$  of matrix  $B_{n,r}$  on the reconstruction

quality.  $n = 300$

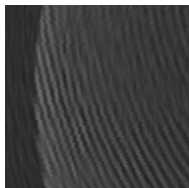


Plot of Mean Square Error as a function of rank  $r$ .

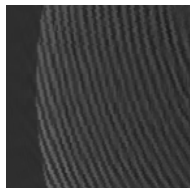
# Experiments and Results: Choosing Rank



(a)  $r = n/3$



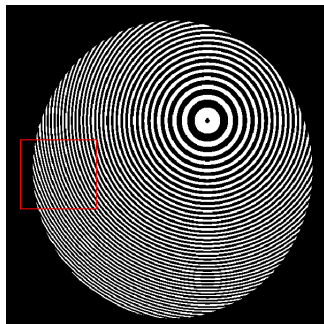
(b)  $r = n/2$



(c)  $r = 9n/10$



(d)  $r = n$

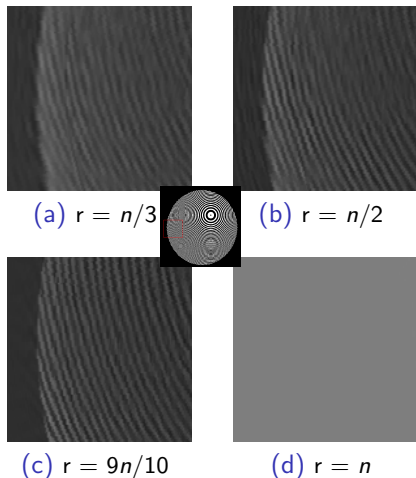


original phantom (f) used in experiments where region to be zoomed is shown in red.

Effect of rank  $r$  of matrix  $B_{n,r}$  on the reconstruction

quality.  $n = 300$

# Experiments and Results: Choosing Rank



Based on our experiments, as a rule of thumb, dropping highest 10% of singular values gives a fairly stable reconstruction.

Effect of rank  $r$  of matrix  $B_{n,r}$  on the reconstruction

quality.  $n = 300$

# Reconstruction In Limited View Scenario

How to remove the artifacts which arise in the Circular arc Radon transform due to the limited view?

# Reconstruction of Singularities under Radon Transforms.

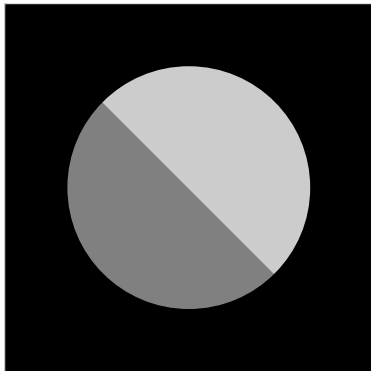


**Figure:** Image with visualization of projection value along direction shown.

# Reconstruction of Singularities under Radon Transforms.

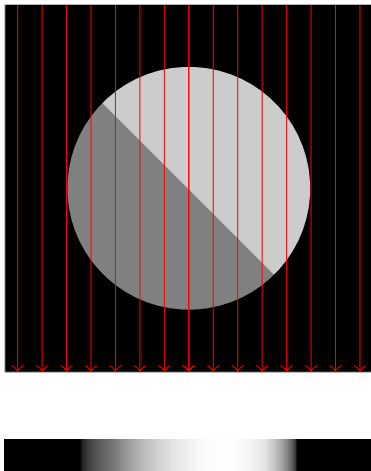


**Figure:** Image with visualization of projection value along direction shown.

# Reconstruction of Singularities under Radon Transforms.

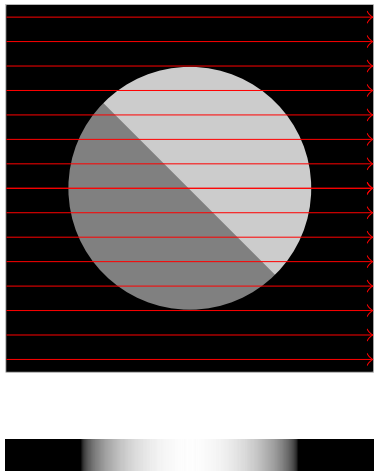


**Figure:** Image with visualization of projection value along direction shown.

# Reconstruction of Singularities under Radon Transforms.

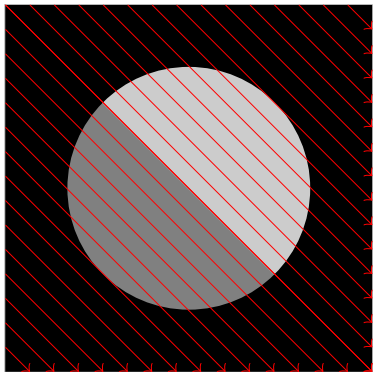


**Figure:** Image with visualization of projection value along direction shown.

# Reconstruction of Singularities under Radon Transforms.

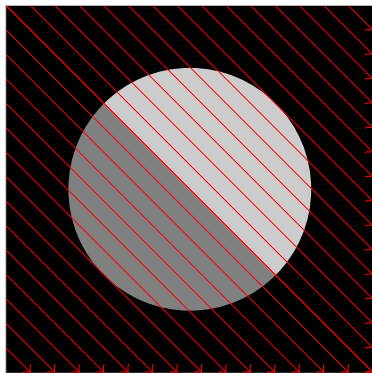


**Figure:** Image with visualization of projection value along direction shown.

Let  $\mathcal{C}$  be the set of curves, along which we measure projections. Then for an edge to be visible there must be at least one element in the interior of set  $\mathcal{C}$ , tangential to the edge

# Effect of limited view

- Due to limited view **not all edges are visible**, in the sense of meeting tangency criterion w.r.t set  $\mathcal{C}$ .

# Effect of limited view

- Due to limited view **not all edges are visible**, in the sense of meeting tangency criterion w.r.t set  $\mathcal{C}$ .
- The end points of the arc lie inside the object, which leads to curves  $\mathcal{C}$  having **discontinuities at end points**.

# Effect of limited view

- Due to limited view **not all edges are visible**, in the sense of meeting tangency criterion w.r.t set  $\mathcal{C}$ .
- The end points of the arc lie inside the object, which leads to curves  $\mathcal{C}$  having **discontinuities at end points**.
- The presence of these sharp discontinuities in data set  $\mathcal{C}$  and limited view will lead to **streak and circular artifacts**.

# Effect of limited view

- Due to limited view **not all edges are visible**, in the sense of meeting tangency criterion w.r.t set  $\mathcal{C}$ .
- The end points of the arc lie inside the object, which leads to curves  $\mathcal{C}$  having **discontinuities at end points**.
- The presence of these sharp discontinuities in data set  $\mathcal{C}$  and limited view will lead to **streak and circular artifacts**.

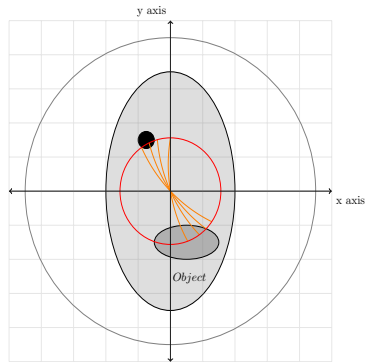


**Figure:** A sharp circular artifact is observed due to discontinuity in angular, as well as radial direction

# Reducing artifacts in reconstructed images

- To reduce the artifacts in the reconstructed images we smooth out the discontinuities of the elements of  $\mathcal{C}$

# Reducing artifacts in reconstructed images

- To reduce the artifacts in the reconstructed images we smooth out the discontinuities of the elements of  $\mathcal{C}$
- This is achieved by gracefully decaying arcs to zero at the edges.

# Reducing artifacts in reconstructed images

- To reduce the artifacts in the reconstructed images we smooth out the discontinuities of the elements of  $\mathcal{C}$
- This is achieved by gracefully decaying arcs to zero at the edges.
- Algorithmically, this achieved by weighing rows of  $B_n$  by a factor of the form  $e^{-\frac{(i-h)^2}{\sigma^2}}$ ; visualized below.

# Reducing artifacts in reconstructed images

- To reduce the artifacts in the reconstructed images we smooth out the discontinuities of the elements of  $\mathcal{C}$
- This is achieved by gracefully decaying arcs to zero at the edges.
- Algorithmically, this is achieved by weighing rows of  $B_n$  by a factor of the form  $e^{-\frac{(i-h)^2}{\sigma^2}}$ ; visualized below.

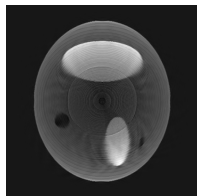


Visualization of structure of unmodified original matrix  $B_n$ .

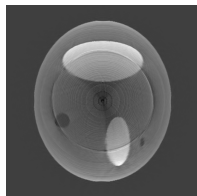


Visualization of structure of modified matrix  $B_n$  for artifact suppression.

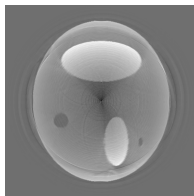
# Experiments and Results: Artifact Reduction.



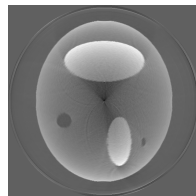
(a)  $\alpha = 21$



(b)  $\alpha = 31$

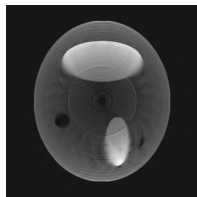


(c)  $\alpha = 46$

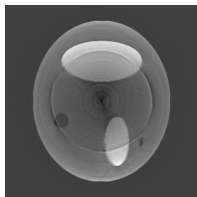


(d)  $\alpha = 76$

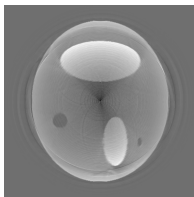
# Experiments and Results: Artifact Reduction.



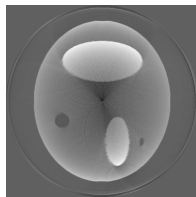
(a)  $\alpha = 21$



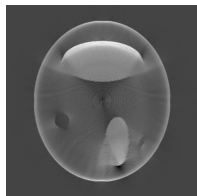
(b)  $\alpha = 31$



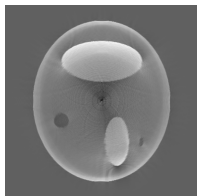
(c)  $\alpha = 46$



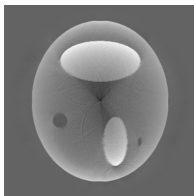
(d)  $\alpha = 76$



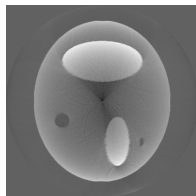
(e)  $\alpha = 21$



(f)  $\alpha = 31$



(g)  $\alpha = 46$



(h)  $\alpha = 76$

Reconstructed images corresponding to different  $\alpha$  before (row 1), and after artifact suppression (row 2).

# Experiments and Results: Artifact Reduction

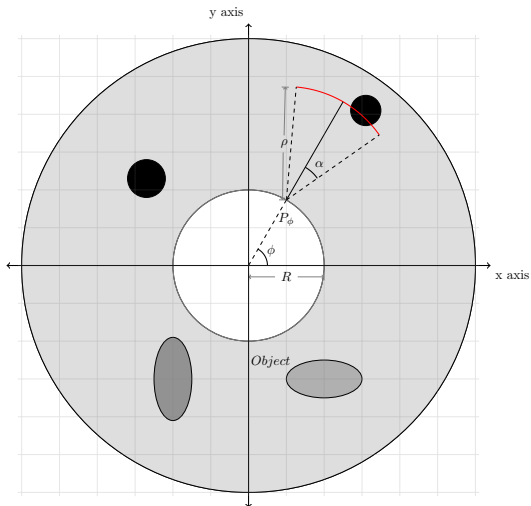
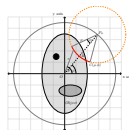


Figure: Setup with support outside the acquisition circle

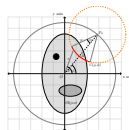
# Experiments and Results: Artifact Reduction

$$g_n^\alpha(\rho) = \int_{\sqrt{R^2 + \rho^2 + 2\rho R \cos \alpha} - R}^{\rho} \frac{K_n(\rho, u)}{\sqrt{\rho - u}} F_n(u) du$$

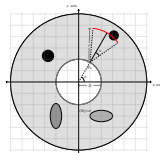


# Experiments and Results: Artifact Reduction

$$g_n^\alpha(\rho) = \frac{\rho}{\sqrt{R^2 + \rho^2 + 2\rho R \cos \alpha} - R} \frac{K_n(\rho, u)}{\sqrt{\rho - u}} F_n(u) du$$



$$g_n^\alpha(\rho) = \frac{\rho}{R - \sqrt{R^2 + \rho^2 - 2\rho R \cos \alpha}} \frac{K_n(\rho, u)}{\sqrt{\rho - u}} F_n(u) du$$



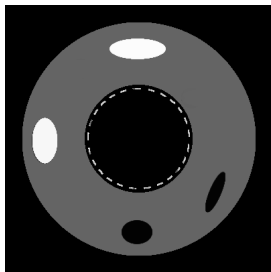
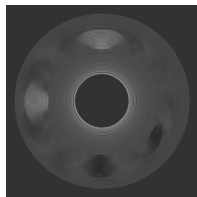
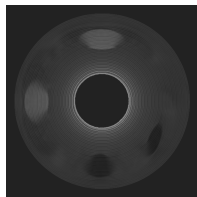


Figure: Phantom with support outside the acquisition circle.

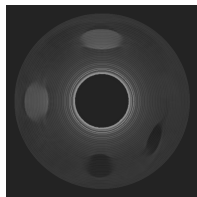
# Experiments and Results: Artifact Reduction



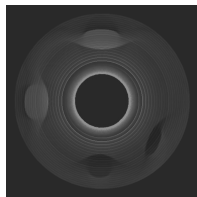
(a)  $\alpha = 21$



(b)  $\alpha = 31$



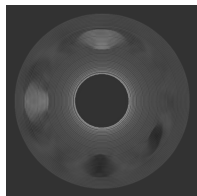
(c)  $\alpha = 46$



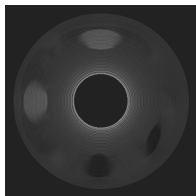
(d)  $\alpha = 76$

Figure: Reconstructed images corresponding to different  $\alpha$  before (row 1), and after artifact

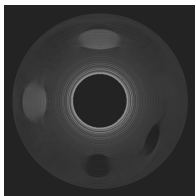
# Experiments and Results: Artifact Reduction



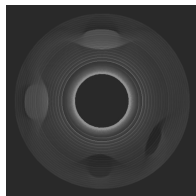
(a)  $\alpha = 21$



(b)  $\alpha = 31$



(c)  $\alpha = 46$



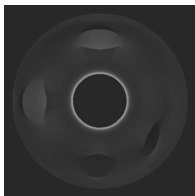
(d)  $\alpha = 76$



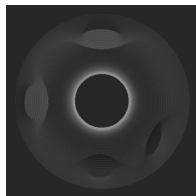
(e)  $\alpha = 21$



(f)  $\alpha = 31$



(g)  $\alpha = 46$



(h)  $\alpha = 76$

Figure: Reconstructed images corresponding to different  $\alpha$  before (row 1), and after artifact reduction (row 2).

# Summary & Future Work.

- ✓ We Proposed a method of numerical inversion of circular arc Radon transform, a limited view generalization of circular Radon transform.

# Summary & Future Work.

- ✓ We Proposed a method of numerical inversion of circular arc Radon transform, a limited view generalization of circular Radon transform.
- ✓ We also proposed a strategy to reduce the artifacts which arise in the image due to limited view.

# Summary & Future Work.

- ✓ Provide a rigorous mathematical justification of the artifacts.

# Summary & Future Work.

- ✓ Provide a rigorous mathematical justification of the artifacts.
- ✓ Derive a closed form solution of the Volterra integral equation arising in the transform.

- *PET Image Reconstruction And Denoising On Hexagonal Lattices.*  
**Syed T. A.** and Sivaswamy J.  
International Conference on Image Processing(ICIP) 2015, Quebec city.
- *Numerical inversion of circular arc Radon transform*  
**Syed T. A.**, Krishnan V. P. and Sivaswamy J.  
(Under review).

# Thank You